The effect of gravity and dimensionality on the impact of cylinders and spheres onto a wall in a viscous fluid

Acmae El Yacoubi, Sheng Xu, and Z. Jane Wang

Citation: Physics of Fluids **29**, 020717 (2017); doi: 10.1063/1.4974519
View online: http://dx.doi.org/10.1063/1.4974519
View Table of Contents: http://aip.scitation.org/toc/phf/29/2
Published by the American Institute of Physics

PHYSICS OF FLUIDS **29**, 020717 (2017)

The effect of gravity and dimensionality on the impact of cylinders and spheres onto a wall in a viscous fluid

Acmae El Yacoubi,[1] Sheng Xu,[2] and Z. Jane Wang[1,a)]
[1]*Department of Mechanical and Aerospace Engineering, Cornell University, Ithaca, New York 14853, USA*
[2]*Department of Mathematics, Southern Methodist University, Dallas, Texas 75275-0156, USA*

(Received 20 July 2016; accepted 26 December 2016; published online 17 February 2017)

As a solid body approaches a wall in a viscous fluid, the flow in the gap between them is dominated by the viscous effect and can be approximated by the lubrication theory. Here we show that without gravity, a cylinder comes to rest asymptotically at a finite separation from the wall, whereas with gravity, the cylinder approaches the wall asymptotically and contact does not happen in finite time. A cylinder approaches the wall much slower compared to a sphere under matching conditions, implying that the lubrication approximates hold longer before the molecular scale sets in. Our results further serve as a building block for analyzing particle interactions in close proximity, and provide analytic results for integrating the lubrication theory into the computations of Navier-Stokes equations. *Published by AIP Publishing.* [http://dx.doi.org/10.1063/1.4974519]

I. INTRODUCTION

The interaction of particles in fluids is key to understanding collective behavior of particles in particle-laden flows such as sedimentation,[2,6] particle suspensions,[15,17] cloud formation,[8,16] as well as biological phenomena such as ocean biomixing and nutrient transport.[13,14] In the high particle-density limit, close-range particle interactions become an important feature of such flows. They introduce small length and time scales in the otherwise inertia-dominated flows.

One question about the interaction of two particles in a fluid is whether they bounce off each other or will they stick together? Unlike dry collisions, the dynamics of two particles approaching each other is dictated by lubrication force when the gap between them is small. The classical lubrication theory predicts that contact and rebound of two particles would not be possible because the hydrodynamic force diverges as the gap separation tends to zero.[1,7] A key parameter in studying particle collisions in fluids is the Stokes number. It is defined as the ratio of the particle inertia to the Stokes drag. More recent experimental and theoretical studies[3–5,11,12,22] have shown that there is no contact or rebound if the Stokes number is less than critical values, but contact and rebound can occur if the Stokes number is sufficiently high. The classical lubrication theory needs to be augmented to account for the effects of the compressibility and non-continuum of fluids[5] and the deformation and roughness of particles[3,4,10] to make contact and rebound possible at high Stokes numbers. When the Stokes number is low, the particle inertia is small relative to the viscous drag, and the kinetic energy of the particle cannot compensate for the viscous dissipation. So particles approaching each other by inertia slow down and come to rest at a given separation, and no contact or rebound is to take place.

In this paper, we apply the lubrication theory to study the dynamics of a cylinder approaching a wall in a viscous fluid with or without gravity. We present numerical solutions of the dynamics at different key parameters. We show that without gravity, the cylinder comes to rest asymptotically at a finite separation from the wall, and contact does not happen; and with gravity, a constant force driving the cylinder toward the wall, the cylinder approaches the wall asymptotically, but contact does not happen in finite time. These results hold in both 2D and 3D. We compare the dynamics of the cylinder with a sphere and show that the continuum limit for the cylinder holds for a larger range of the Stokes number and, under matching conditions, a longer time than the sphere.

Our analysis was further motivated by our interest in computing the full Navier-Stokes solutions of particles colliding in unsteady flows. Collisions between particles introduce numerical difficulties in resolving the flow. Instead of using brute-force methods of refining grid spacing or introducing ad-hoc collision rules, we can integrate the lubrication theory within Navier-Stokes solvers. The results presented here provide explicit solutions for the development of such methods.

II. MODELS

We consider the case of a cylinder falling vertically toward a fixed wall in an incompressible viscous fluid, as illustrated in Figure 1.

The flow around the cylinder is governed by the Navier-Stokes equations

$$\frac{\partial \vec{v}}{\partial t} + \vec{v} \cdot \nabla \vec{v} = -\nabla p + \nu^* \nabla^2 \vec{v}, \tag{1a}$$

$$\nabla \cdot \vec{v} = 0, \tag{1b}$$

where $\vec{v} = (u, v)$ is the fluid velocity, p is the fluid pressure, and ν^* is the non-dimensional kinematic viscosity of the fluid.

a)Author to whom correspondence should be addressed. Electronic mail: jane.wang@cornell.edu. Tel.: +1 607 255 5354. Also at Department of Physics, Cornell University, Ithaca, NY 14853, USA.

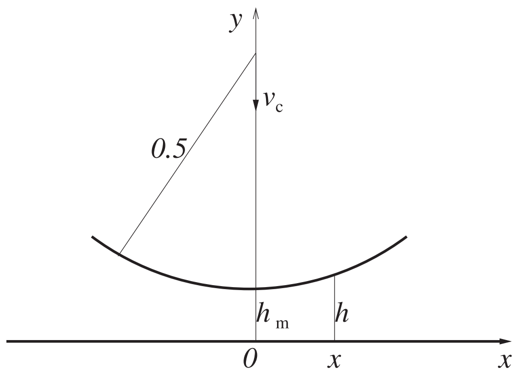

FIG. 1. Sketch of a cylinder falling vertically toward a fixed wall. v_c is the falling velocity, h is the height at position x, and h_m is the minimum gap height at $x = 0$.

Hereafter, all variables and quantities are non-dimensionalized with the cylinder diameter $\mathtt{D}$, the initial falling speed of the cylinder $\mathtt{v}_{c,0}$, and the fluid density $\rho_{\mathtt{f}}$ unless otherwise specified. So $\nu^* = \mu_{\mathtt{f}}/(\rho_{\mathtt{f}}\mathtt{v}_{c,0}\mathtt{D})$, where $\mu_{\mathtt{f}}$ is the dynamic viscosity of the fluid.

When the cylinder is in close proximity to the wall, the flow in the gap between the cylinder and the wall can be approximated by the lubrication equations[21]

$$\frac{\partial u}{\partial x} + \frac{\partial v}{\partial y} = 0, \tag{2a}$$

$$\frac{\partial^2 u}{\partial y^2} = \frac{1}{\nu^*}\frac{dp}{dx}. \tag{2b}$$

Equation (2b) is valid when $h_m \ll 1$ and $h_m^2/\nu^* \ll 1$, where h_m is the minimum gap clearance in the wall-normal direction (non-dimensionalized by the diameter of the cylinder $\mathtt{D}$). These are the two conditions for the lubrication theory to hold. At this lubrication limit, the flow in the gap can be considered as quasi-steady. Equations (2b) and (2a) can be integrated to give

$$u = \frac{1}{2\nu^*}\frac{dp}{dx}y(y - h), \tag{3a}$$

$$\frac{dp}{dx} = 12\nu^* v_c \frac{x}{h^3}, \tag{3b}$$

where the height h at the abscissa x is illustrated in Figure 1 and v_c is the vertical velocity (falling velocity) of the cylinder.

The dynamics of the cylinder settling under gravity are governed by the following ordinary differential equation (ODE):

$$m_s\frac{dv_c}{dt} = -(m_s - m_f)g^* + F_f, \tag{4}$$

where $m_s = \pi\gamma/4$ (γ is the cylinder to fluid density ratio) is the mass of the cylinder, $m_f = \pi/4$ is the mass of the displaced fluid, $g^* = \mathtt{g}\mathtt{D}/\mathtt{v}_{c,0}^2$ ($\mathtt{g}$ is the gravitational constant) is the non-dimensional gravitational acceleration, and F_f is the vertical fluid force.

During the lubrication phase, the fluid force F_f is dominated by the contribution from the lubrication region, which can be obtained by integrating the pressure gradient distribution in Equation (3b) twice[9]

$$F_f = -\frac{3\pi\nu^* v_c}{2}h_m^{-3/2}, \tag{5}$$

and Equation (4) becomes

$$\frac{dv_c}{dt} = -\frac{\gamma - 1}{\gamma}g^* - \frac{6\nu^* v_c}{\gamma}h_m^{-3/2}. \tag{6}$$

III. ANALYTIC RESULTS

Since $\frac{dh_m}{dt} = v_c$, Equation (6) can be rewritten as

$$\frac{d^2 h_m}{dt^2} = -\frac{\gamma - 1}{\gamma}g^* - \frac{6\nu^*}{\gamma}h_m^{-3/2}\frac{dh_m}{dt}. \tag{7}$$

We can integrate Equation (7) once with respect to time from $t_0 = 0$ to t to obtain

$$v_c - v_{c,0} = -\frac{\gamma - 1}{\gamma}g^*(t - t_0) + \frac{12\nu^*}{\gamma}\left(\frac{1}{\sqrt{h_m}} - \frac{1}{\sqrt{h_{m,0}}}\right), \tag{8}$$

where $h_{m,0}$ and $v_{c,0} = -1$ are the values of h_m and v_c at time $t_0 = 0$. Replacing v_c by $\frac{dh_m}{dt}$, Equation (8) can be integrated numerically using an ODE solver for $h_m(t)$, which then gives $v_c(t)$ by Equation (8) and the acceleration $a(t) = \frac{dv_c}{dt}$ by Equation (6).

Setting $v_c = 0$ in Equation (8) and denoting the values of h_m and t corresponding to $v_c = 0$ as $h_{m,\infty}$ and t_∞, respectively, we have[21]

$$\frac{h_{m,\infty}}{h_{m,0}} = \frac{1}{\left[1 + \frac{\gamma\sqrt{h_{m,0}}}{12\nu^*}\left(1 + \frac{\gamma-1}{\gamma}g^* t_\infty\right)\right]^2}. \tag{9}$$

With gravity, the cylinder cannot come to rest at a finite distance since otherwise, there would not be a fluid force to balance the weight. Equation (9) states that $t_\infty \to \infty$ as $h_{m,\infty} \to 0$, and the contact cannot occur in finite time.

In the absence of gravity, i.e., without the first term at the right-hand side of Equation (7) and (9) becomes

$$\frac{h_{m,\infty}}{h_{m,0}} = \frac{1}{\left(1 + \frac{\gamma\sqrt{h_{m,0}}}{12\nu^*}\right)^2}, \tag{10}$$

and Equation (7) can be solved analytically with the initial conditions $v_c = -1$ and $h_m = h_{m,0}$ at $t = 0$ to give

$$t = -K(h_m - h_{m,0}) - 2KH_0(\sqrt{h_m} - \sqrt{h_{m,0}}) - 2KH_0^2\ln\left(\frac{\sqrt{h_m} - H_0}{\sqrt{h_{m,0}} - H_0}\right), \tag{11}$$

where $K = \frac{S\sqrt{h_{m,0}}}{12+S\sqrt{h_{m,0}}}$ and $H_0 = \frac{12\sqrt{h_{m,0}}}{12+S\sqrt{h_{m,0}}}$ with $S = \gamma/\nu^*$. The parameter $S = \gamma/\nu^* = 4\mathtt{m}_s\mathtt{v}_{c,0}/(\pi\mu_{\mathtt{f}}\mathtt{D})$ ($\mathtt{m}_s = \gamma\rho_{\mathtt{f}}\pi\mathtt{D}^2/4$ and $\mathtt{v}_{c,0}$ are the dimensional mass and initial speed of the cylinder) for the cylinder in 2D. It is like the Stokes number for a sphere in 3D. It characterizes the magnitude of the inertia of the cylinder relative to the viscous force on the cylinder. Equation (10) states that $h_{m,\infty}$ (the value of h_m when $v_c = 0$) is finite and is a decreasing function of S. Equation (11) implies that $\sqrt{h_m} \to H_0$ as $t \to \infty$. Note that Equation (10) implies that $h_{m,\infty}$ is finite and is a decreasing function of S. Moreover, Equation (11) implies that it takes infinitely long to approach this finite distance, since $\sqrt{h_m} \to H_0$ as $t \to \infty$.

IV. NUMERICAL SOLUTIONS

The dynamics of the cylinder approaching the wall are described by the minimum gap height $h_m(t)$, the approaching velocity $v_c(t)$ and the approaching acceleration $a_c(t)$ as functions of the time t. The controlling parameters are γ and $S = \gamma/\nu^*$ in the presence of gravity and only $S = \gamma/\nu^*$ in the absence of gravity. The dynamics are also affected by the initial minimum gap $h_{m,0}$ and g^*. Note that $\sqrt{1/g^*} = \mathrm{v}_{c,0}/\sqrt{\mathrm{gD}}$ is the initial falling speed of the cylinder non-dimensionalized by $\sqrt{\mathrm{gD}}$. In our investigations below, we fix $g^* = 1$.

We use the ODE solver ode45 in Matlab to numerically integrate Equation (8) to obtain h_m, v_c, and a_c. Without gravity, we can obtain their analytical results using Equation (11). The ODE solver is validated by comparing numerical and analytical results for a non-gravity case, as shown in Figure 2. Since $v_c \to 0$ as $t \to \infty$, the numerical solver works until v_c is at the level of roundoff error, which occurs at large t as in Figure 2.

A. The effect of gravity

We first investigate the role of gravity on the dynamics of a settling cylinder. To contrast the two cases, we use relatively large values for $S = \gamma/\nu^*$ and γ (but keep $h_m \ll 1$ and $h_m^2/\nu^* \ll 1$) to reduce the effect of the viscous force and to enhance the effect of the gravitational force.

Figure 3 compares the time history of the gap height, velocity, and acceleration of the cylinder in the presence and in the absence of gravity with the same controlling parameters ($\nu^* = 0.005$ and $\gamma = 10$) and initial conditions. At a given time t, the gap height is smaller in the presence of gravity, as gravity pulls the cylinder toward the wall. The numerical solutions in Figure 3 are consistent with the analytical results in Section III. With gravity, h_m decreases with time and approaches 0 as $t \to \infty$, and the contact cannot occur in finite time. Without gravity, h_m approaches a finite positive value as $t \to \infty$, and the contact ($h_m = 0$) does not happen.

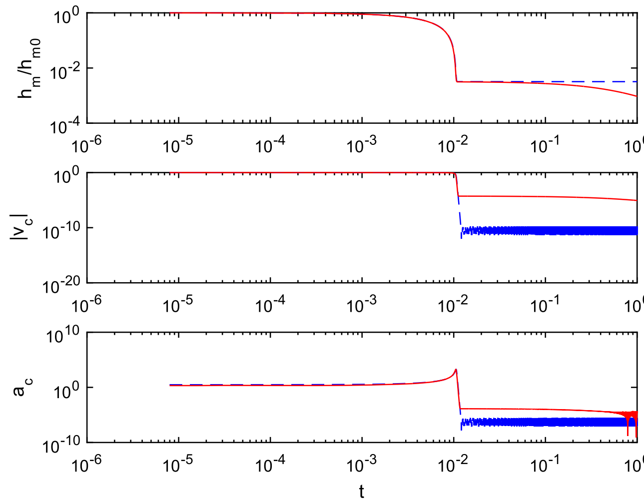

FIG. 3. Time history of the gap height, velocity, and acceleration of a cylinder approaching a wall in the presence (solid, red) and in the absence (dashed, blue) of gravity. $\nu^* = 0.005$, $\gamma = 10$, and $h_{m,0} = 0.01$.

Without the gravity, the only controlling parameter for the dynamics of the cylinder is $S = \gamma/\nu^*$. Figure 4 shows the dynamics in the absence of gravity as we vary $S = \gamma/\nu^*$ but with the same initial condition. It shows that the higher S, the smaller the gap height h_m is at a given time t; and the abrupt change of v_c with t is delayed as S increases. The parameter $S = \gamma/\nu^*$ characterizes the magnitude of the inertia of the cylinder relative to the viscous force on the cylinder. At a larger S, the inertia dominates for a longer time before the viscous force takes over, and the cylinder gets slowed down at later time, which explains the delay of the abrupt change of v_c. The effects of initial gap height on the dynamics of the cylinder in the absence of gravity are shown in Figure 5.

B. Comparison of a cylinder and a sphere

We next compare the dynamics of a cylinder and a sphere. We analyze the dynamics of a sphere approaching awall in

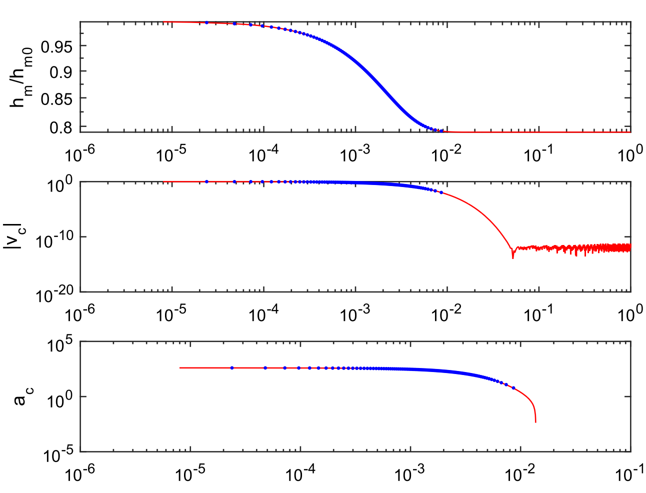

FIG. 2. Comparisons between numerical and analytical results of the gap height, velocity, and acceleration of a cylinder falling vertically toward a fixed wall without gravity. $\nu^* = 0.1$, $\gamma = 1.5$, and $h_{m,0} = 0.01$.

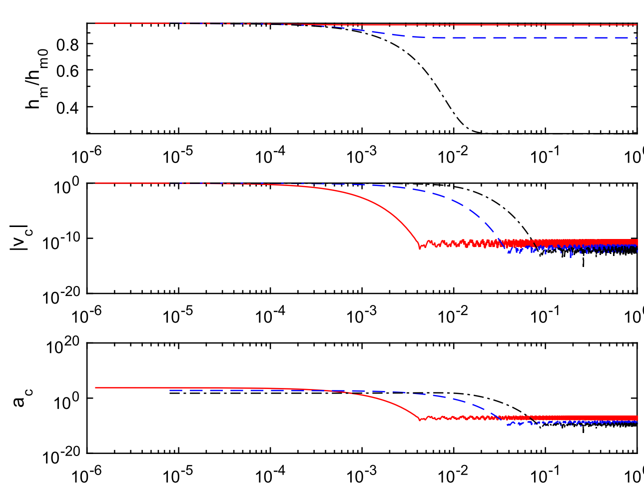

FIG. 4. Time history of the gap height, velocity, and acceleration of a cylinder approaching a wall in the absence of gravity with $h_{m,0} = 0.01$ at different values of $S = \gamma/\nu^*$. $S = 1$: solid, red; $S = 10$: dashed, blue; $S = 100$: dash-dotted, black.

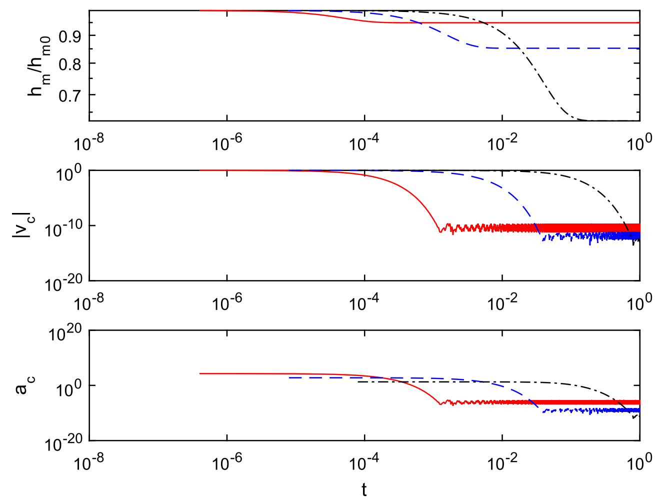

FIG. 5. Time history of the gap height, velocity, and acceleration of a cylinder approaching a wall at $S=\gamma/\nu^*=10$ in the absence of gravity with different initial gap height $h_{m,0}$. $h_{m,0}=0.001$: solid, red; $h_{m,0}=0.01$: dashed, blue; $h_{m,0}=0.1$: dash-dotted, black.

a similar manner as a cylinder. We now use the diameter D of the sphere as the length scale. Under the lubrication limit, the dynamics of the sphere is governed by the following ODE:[21]

$$m_s\frac{dv_c}{dt} = -(m_s-m_f)g^* - \frac{3\pi\nu^* v_c}{2h_m}, \tag{12}$$

where $m_s=\gamma\pi/6$ is the non-dimensional mass of the sphere, $m_f=\pi/6$ is the non-dimensional mass of the displaced fluid, and the fluid force is inversely proportional to h_m.[1] Equation (12) can be written in terms of h_m as

$$\frac{d^2h_m}{dt^2} = \frac{\gamma-1}{\gamma} - \frac{9\nu^*}{\gamma}h_m^{-1}\frac{dh_m}{dt}, \tag{13}$$

which can be integrated once with respect to time t to obtain

$$v_c - v_{c,0} = -\frac{\gamma-1}{\gamma}(t-t_0) - \frac{9\nu^*}{\gamma}\ln\left(\frac{h_m}{h_{m,0}}\right), \tag{14}$$

where $h_{m,0}$ and $v_{c,0}=-1$ are the initial gap height and velocity of the sphere at time $t_0=0$. To get the gap height $h_{m,\infty}$ when the sphere comes to rest, we set $v_c=0$ in Equation (14) and obtain[21]

$$\frac{h_{m,\infty}}{h_{m,0}} = e^{-St(1+\frac{\gamma-1}{\gamma}t_\infty)}, \tag{15}$$

where $St=S/9=2\mathtt{m}_\mathtt{s}\mathtt{v}_{\mathtt{c},0}/(3\pi\mu_\mathtt{f}\mathtt{D}^2)$ ($S=\gamma/\nu^*$ as before, and $\mathtt{m}_\mathtt{s}=\gamma\rho_\mathtt{f}\pi\mathtt{D}^3/6$ and $\mathtt{v}_{\mathtt{c},0}$ are the dimensional mass and initial speed of the sphere) is the Stokes number of the sphere, which is defined as the ratio of the particle inertia to the Stokes drag on the particle.

In the absence of the gravity, we have

$$\frac{h_{m,\infty}}{h_{m,0}} = e^{-St}. \tag{16}$$

Equations (10) and (16) state that in the absence of gravity, $h_{m,\infty}/h_{m,0}$ decays algebraically with $S=\gamma/\nu^*$ and is dependent on the initial gap height $h_{m,0}$ for a cylinder, while exponentially with $S=9St$ and independent of $h_{m,0}$ for a sphere. Figure 6 shows the comparison of a cylinder and a sphere in terms

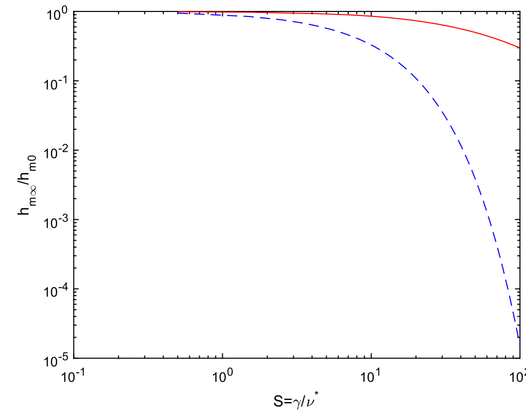

FIG. 6. Dependence of $h_{m,\infty}/h_{m,0}$ on $S=\gamma/\nu^*$ for a cylinder and a sphere. Cylinder: solid, red; sphere: dashed, blue. $h_{m,0}=0.01$ for the cylinder.

of the dependence of $h_{m,\infty}/h_{m,0}$ on $S=\gamma/\nu^*$. For a cylinder, it takes a much larger S before micro-scale effects (surface roughness, van der Waals forces, and non-continuum effects) set in. As such, the lubrication approximations for a cylinder are valid for a larger range of density ratios and kinematic viscosity.

In Figure 7 we compare the dynamics of a cylinder and a sphere approaching a wall in the presence of gravity with the same γ, ν^*, and initial conditions. For a cylinder, it takes much longer time before micro-scale effects set in, and the lubrication approximations for a cylinder is valid for a longer time.

C. Simulations of full dynamics with lubrication theory incorporated to handle the collision

We have developed a flow simulation method to couple the dynamics of a fluid and moving particles in both the inertia and lubrication phases of the particles. The underlying direct numerical simulation method is the immersed interface method,[18–20] which enforces boundary conditions by singular forces at the boundaries of particles. In the inertia

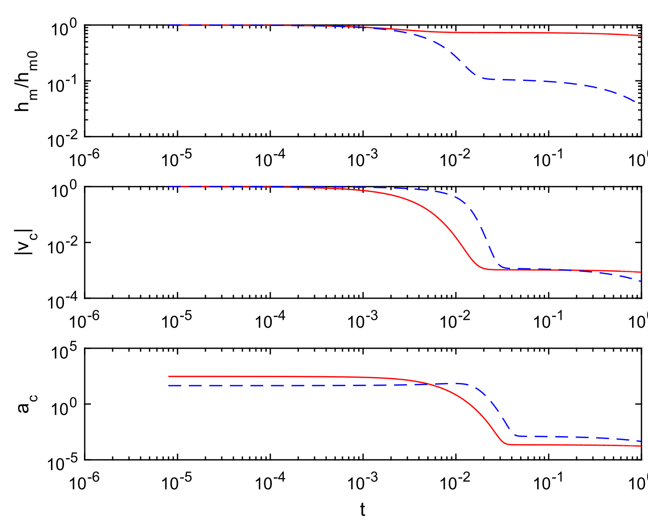

FIG. 7. Comparison of the dynamics of a cylinder and a sphere approaching a wall in the presence of gravity in terms of the time history of the gap height, velocity, and acceleration. Cylinder: solid, red; sphere: dashed, blue. $\gamma=2$, $\nu^*=0.1$, $h_{m,0}=$ 0.01.

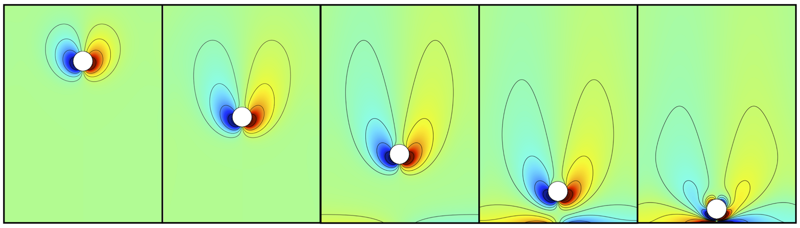

FIG. 8. Vorticity contours around a cylinder settling in a viscous fluid under gravity toward a fixed wall from the numerical simulation by the immersed interface method. $\gamma = 1.5$.

phase when a particle is away from the others, a boundary-condition-capturing strategy[20] is used to numerically determine the singular forces. When two particles are in close proximity, we use the lubrication approximations to analytically determine the singular forces in the lubrication region. Detailed description and validation of the method will be reported elsewhere.

Figure 8 shows the vorticity contours around a cylinder settling under gravity toward a fixed wall. The flow is in the inertia regime in the first four snapshots, and in the lubrication regime in the last one.

V. CONCLUSIONS

We investigated the dynamic behavior of a cylinder approaching a wall in a viscous fluid. We showed that without gravity, the cylinder comes to rest asymptotically at a finite separation from the wall, and contact does not occur, while if there is gravity, the cylinder approaches the wall as time goes to infinity. We found that when the initial inertia of the cylinder is high relative to the viscous fluid force, the falling speed is quickly damped.

We compared the dynamics of a cylinder in 2D with a sphere in 3D. The above conclusions for a cylinder in 2D also apply to a sphere in 3D. The main difference lies in the rates of decay. Without gravity, the asymptotic gap height decays with the Stokes number algebraically for a cylinder while exponentially for a sphere. Additionally, the gap height for a cylinder decreases with time slower than a sphere under the same conditions with or without gravity. So the lubrication theory holds valid for a longer time and a wider range of parameters in the case of a cylinder before the breakdown by micro-scale effects.

Finally, we showed that the lubrication approximations can be incorporated into a Navier-Stokes simulation to couple the dynamics of the fluid and particles in both inertia-dominant regime and viscosity-dominant regime. This offers a computational tool for examining a large range of phenomena involving particle collisions at finite Reynolds numbers.

ACKNOWLEDGMENTS

Below are two personal tributes to Professor John Lumley by S.X. and Z.J.W.

S.X.: I once received a letter from Hillary Clinton's office when she was a New York senator. The story of the letter dates back to 2001. Right before the start of a group meeting in the fall semester of that year, Professor Lumley asked me about my wife, as he knew I got married lately in the summer. After he learned that my wife could not join me because she did not get the visa, he said he could write to a senator to ask for help and joked that "need help? ask a senator." He never mentioned this again, and I did not follow up on it either. I later forgot about it as my wife soon got her visa. One day in early 2002, a letter came to my surprise, and it was the reply from Hillary Clinton's office to Professor Lumley's request for help with my wife's visa application. I feel moved by this story whenever I think of it. I was very fortunate to have Professor Lumley as my adviser, a world-renowned scientist and a great human being.

Z.J.W.: I had a few exchanges with John Lumley during his later years at Cornell. Each exchange was brief, yet each had an impact. Shortly after I arrived at Cornell, he asked me to contribute an article to the Annual Review of Fluid Mechanics on the subject of insect flight that I had been working on. It set me to work intensely for about two years, combing through my thoughts and the literature on the subject.

In another conversation, he pointed out to me that when a drop of milk falls in water, it forms a cascade of ring-like structures. He wondered whether such a formation had something to do with vortices shed behind the drops. We mused on various possibilities. As I recall, there was a sparkle in his eyes when he was thinking the problem aloud. The elementary problem studied in this paper constitutes a building block for a general computational method we are developing to simulate multiple particles falling in intermediate Reynolds number flows. It occurs to me now as I am writing this tribute that the method would be ideally suited to answering the question John Lumley asked many years ago.

S.X. thanks NSF for the support of his work under Grant No. NSF DMS 1320317.

[1] M. D. A. Cooley and M. E. O'Neill, "On the slow motion generated in a viscous fluid by the approach of a sphere to a plane wall or a stationary sphere," Mathematica **16**, 37–49 (1969).

[2] W. B. Daniel, R. E. Ecke, G. Subramanian, and D. L. Koch, "Clusters of sedimenting high-Reynolds-number particles," J. Fluid Mech. **625**, 371–385 (2008).

[3] R. H. Davis, J.-M. Serayssol, and E. J. Hinch, "The elastohydrodynamic collision of two spheres," J. Fluid Mech. **163** 479–497 (1986).

[4] R. H. Davis, "Effects of surface roughness on a sphere sedimenting through a dilute suspension of neutrally buoyant spheres," Phys. Fluids A **4**(12), 2607–2619 (1992).
[5] A. Gopinath, S. B. Chen, and D. Koch, "Lubrication flows between spherical particles colliding in a compressible non-continuum gas," J. Fluid Mech. **344**, 245–269 (1997).
[6] É. Guazzelli and J. Hinch, "Fluctuations and instability in sedimentation," Annu. Rev. Fluid Mech. **43**, 97–116 (2011).
[7] L. M. Hocking, "The effect of slip on the motion of a sphere close to a wall and of two adjacent spheres," J. Eng. Math. **7**(3), 207–221 (1973).
[8] P. J. Ireland and L. R. Collins, "Direct numerical simulation of inertial particle entrainment in a shearless mixing layer," J. Fluid Mech. **704**, 301–332 (2012).
[9] D. J. Jeffrey and Y. Onishi, "The slow motion of a cylinder next to a plane wall," Q. J. Mech. Appl. Math. **34**(2), 129–137 (1981).
[10] J. T. Jenkins and M. A. Koenders, "Hydrodynamic interaction of rough spheres," Granular Matter **7**, 13–18 (2005).
[11] G. G. Joseph, R. Zenit, M. L. Hunt, and A. M. Rosenwinkel, "Particle-wall collisions in a viscous fluid," J. Fluid Mech. **433**, 329–346 (2001).
[12] G. G. Joseph and M. L. Hunt, "Oblique particle-wall collisions in a liquid," J. Fluid Mech. **510**, 71–93 (2004).
[13] K. Katija and J. O. Dabiri, "A viscosity-enhanced mechanism for biogenic ocean mixing," Nature **460**, 624–627 (2009).
[14] H. Kurtuldu, J. S. Guasto, K. A. Johnson, and J. P. Gollub, "Enhancement of biomixing by swimming algal cells in two-dimensional films," Proc. Natl. Acad. Sci. U. S. A. **108**(26), 10391–10395 (2011).
[15] N.-Q. Nguyen and A. J. C. Ladd, "Lubrication corrections for lattice-Boltzmann simulations of particle suspensions," Phys. Rev. E **66**, 046708 (2002).
[16] Z. Warhaft, "Laboratory studies of droplets in turbulence: Towards understanding the formation of clouds," Fluid Dyn. Res. **41**, 011201 (2009).
[17] J. J. Wylie and D. L. Koch, "Particle clustering due to hydrodynamic interactions," Phys. Fluids **12**(5), 964–970 (2000).
[18] S. Xu and Z. J. Wang, "An immersed interface method for simulating the interaction of a fluid with moving boundaries," J. Comput. Phys. **216**, 454–493 (2006).
[19] S. Xu and Z. J. Wang, "Systematic derivation of jump conditions for the immersed interface method in three-dimensional flow simulation," SIAM J. Sci. Comput. **27**(6), 1948–1980 (2006).
[20] S. Xu, "The immersed interface method for simulating prescribed motion of rigid objects in an incompressible viscous flow," J. Comput. Phys. **227**, 5045–5071 (2008).
[21] A. Yacoubi, "Particle hydrodynamic interactions in intermediate Reynolds number flows," Ph.D. dissertation (Cornell University, 2013).
[22] F.-L. Yang and M. L. Hunt, "Dynamics of particle-particle collisions in a viscous liquid," Phys. Fluids **18**(12), 121506 (2006).